

Telechelic all-*cis* polycyclooctene *via* catalytic stereoretentive ROMP for the synthesis of polylactide-based ABA triblock copolymers†

Jake L. Nicholson,^a Antoine C. Gravet^a and Quentin Michaudel  ^{*ab}

Received 3rd May 2025, Accepted 8th May 2025

DOI: 10.1039/d5fd00067j

Polylactide (PLA) is a commercial and sustainably sourced aliphatic polyester but its applications have been limited by its low toughness. The insertion of a rubbery segment within the PLA backbone is among the promising strategies to enhance the mechanical properties of PLA while retaining sustainability. Herein, we disclose a catalytic stereoretentive ring-opening metathesis polymerization process to access high molar mass (M_n^{exp} up to 127.9 kg mol⁻¹) all-*cis* telechelic polycyclooctene (PCOE) at low catalyst loadings. The use of *cis*-1,4-diacetoxy-2-butene as a chain-transfer agent in the presence of stereoretentive dithiolate Ru carbenes afforded precise control over the *cis* content, the molar mass, and the introduction of acetoxy chain ends. Subsequent hydrolysis of the acetoxy motifs followed by chain extension *via* ring-opening polymerization of D,L-lactide yielded high molar mass (M_n^{exp} up to 105.0 kg mol⁻¹) all-*cis* PLA ABA triblock copolymers. The influence of the molar mass of the all-*cis* PCOE over the thermal and mechanical properties of the ABA triblock was investigated.

Introduction

Designing sustainable polymeric materials is a critical step toward addressing the global plastic waste crisis. To meet this challenge, new design principles that emphasize embedded recyclability, the use of biorenewable monomers, in addition to high mechanical and thermal performance are essential. This quest for sustainable polymers has driven the investigation of materials with ever-increasing molecular complexity compared to current high-commodity plastics. For example, precise control of polymer stereochemistry has been shown to be crucial to control not only the material's properties, but also degradation rates and overall recyclability, which are crucial factors for realizing a circular materials

^aDepartment of Chemistry, Texas A&M University, College Station, Texas, 77843, USA. E-mail: quentin.michaudel@chem.tamu.edu

^bDepartment of Materials Science and Engineering, Texas A&M University, College Station, Texas, 77843, USA

† Electronic supplementary information (ESI) available. See DOI: <https://doi.org/10.1039/d5fd00067j>



economy. Two families of ruthenium carbenes have recently been identified as imparting stereoselectivity during the olefin metathesis process. A *cis*-selective cyclometalated ruthenium catalyst initially developed by the Grubbs group^{1–3} favors the formation of *cis* alkenes from terminal alkenes where stereoretentive dithiolate ruthenium carbenes synthesized by Hoveyda and coworkers^{4,5} maintain the *cis/trans* stereochemistry of the starting material into the product (see Fig. 1a for an overview of the catalysts used in this study). Our group has recently demonstrated the potential of stereoselective olefin metathesis as an effective strategy to tune the physical properties of a broad variety of alkene-containing polymers through the modulation of the *cis/trans* alkene content. A stereoretentive ring-opening metathesis polymerization (ROMP) allowed the synthesis of all-*cis* poly(*p*-phenylene vinylene)s (PPVs) with living characteristics and high molar masses.^{6–9} This strategy leveraged the unique reactivity of dithiolate Ru carbenes to impart a kinetic control over the stereoselectivity for the ROMP and thereby overcome the thermodynamic bias for *trans* alkenes.^{5,10} This stereoretentive catalysis was then implemented into a stereocontrolled acyclic diene metathesis (ADMET) polymerization of *cis,cis*-monomers, where predictable *cis/trans* ratios were accessible through control of the reaction conditions (temperature, reaction time) for a variety of polyalkenamers.¹¹ Shifting to cyclometalated Ru carbenes enabled a *cis*-selective ADMET polymerization, delivering up to 99% *cis* polyalkenamers from readily accessible terminal alkenes.¹² This stereoselective

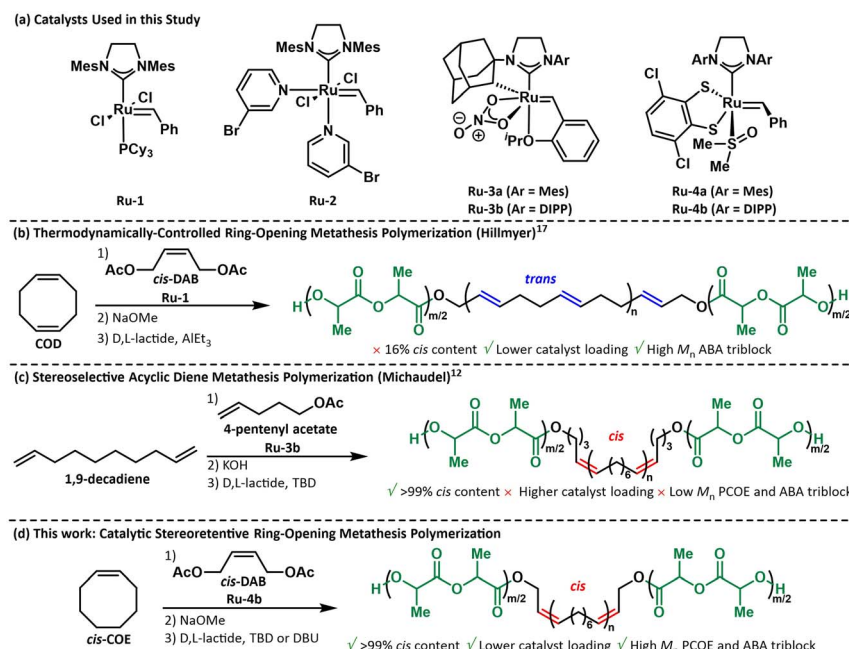


Fig. 1 (a) Overview of catalysts used in this study. (b) Previous work accessing *trans*-rich ABA triblock copolymers through ROMP. (c) Previous work using stereoselective ADMET to synthesize all-*cis* ABA triblock copolymers. (d) Catalytic stereoretentive ROMP developed in this work to access high molar mass all-*cis* PCOE and ABA triblock copolymers at lower catalyst loadings.



ADMET was implemented into the synthesis of all-*cis* polymers with degradable backbones, *e.g.*, polyesters, polycarbonates, and polysiloxanes.

PLA is a recyclable aliphatic polyester most commonly synthesized from ring-opening polymerization (ROP) of lactide, a cyclic dimer of lactic acid which is abundantly produced by fermenting dextrose extracted from renewable agricultural resources such as corn.¹³ Despite successful commercialization, PLA is known to suffer from brittleness which hinders its use in other applications that require mechanical toughness (*i.e.* higher impact strength and/or elongation).¹⁴ While several strategies have been employed to increase its toughness including the addition of plasticizers¹⁵ and polymer blends,¹⁶ the incorporation of a rubbery middle block is an attractive approach to increase the elasticity of PLA first reported by Hillmyer and coworkers (Fig. 1b).¹⁷ While the seminal synthetic route was based on a non-stereoselective ROMP, our ADMET approach enabled synthesis of either a *cis*- or a *trans*-rich middle block to further probe the impact of the *cis/trans* content on the ABA triblock properties (Fig. 1c). The *trans*-rich triblock copolymer (89% *trans*) exhibited a higher glass-transition temperature (T_g) than its all-*cis* counterpart ($T_{g,trans} = 44\text{ }^\circ\text{C}$ vs. $T_{g,cis} = 32\text{ }^\circ\text{C}$) and displayed semi-crystalline behavior, in contrast to the amorphous character of the all-*cis* material. Additionally, although both triblock copolymers had a significantly lower reduced Young's modulus (E_r) compared to native PLA—indicating a lower stiffness of the material—the all-*cis* triblock had the lowest of the series. While this study holds promise for the design of PLA with enhanced properties, the step-growth nature of ADMET limited the molar mass obtained for the middle polyalkenamer block ($M_n = 3.3\text{ kg mol}^{-1}$) and prevented the investigation of the impact of the length of the middle block. Additionally, relatively high loadings were required (1 mol%) for the stereoselective catalyst,¹⁸ which remains more expensive than commonly used Grubbs catalysts.¹⁹

Herein, we report the synthesis of all-*cis* polycyclooctene (PCOE) *via* a catalytic stereoretentive ROMP of *cis*-cyclooctene (**cis**-COE) in the presence of *cis*-1,4-diacetoxy-2-butene (**cis**-DAB), a commercially available chain transfer agent (CTA), and its application toward the synthesis of **PLA-PCOE_{cis}-PLA** triblock copolymers through the preparation of a telechelic middle block with predictable and high molar masses (up to 127.9 kg mol^{-1}). Hydrolysis of the acetoxy chain ends followed by ring-opening polymerization (ROP) of D,L -lactide enabled synthesis of high molar mass all-*cis* ABA triblock copolymers (M_n up to 105.0 kg mol^{-1}). The thermal and mechanical properties of the high molar mass polymers were then compared to those of the smaller analogous polymers previously reported by our group. The ability to synthesize high molar mass polymers at lower catalyst loadings should enable broader adoption of this method for the future development of recyclable plastics with desirable physical properties.

Results and discussion

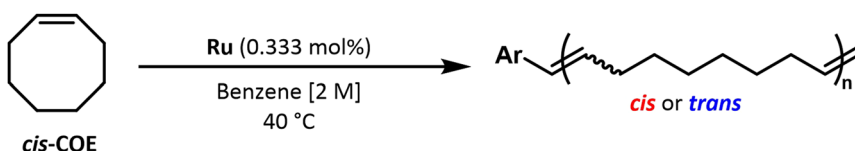
Initial catalyst screen to achieve stereoselective ROMP of *cis*-COE

cis-COE is a low-strain cyclic alkene ($\sim 7.4\text{ kcal mol}^{-1}$) that undergoes ROMP with Grubbs-type catalysts, albeit with typically limited control due to backbiting side reactions and reversible propagation.²⁰ To enable catalyst comparison (Fig. 1a), all polymerizations of **cis**-COE were carried out under a nitrogen atmosphere at $40\text{ }^\circ\text{C}$ in benzene initially using 300 : 1 monomer-to-catalyst loadings. To help reduce



the formation of undesired cyclic oligomers, polymerizations were performed at an increased monomer concentration ($C = 2$ M). As a benchmark of the stereoselectivity, dichloro Grubbs 2nd (**Ru-1**) and 3rd generation (**Ru-2**) delivered PCOE in benzene with low *cis* contents (20% and 16%, respectively) and dispersities over 2 in both cases (Table 1, Entries 1 and 2). Additionally, the discrepancy between theoretical and experimental molar masses determined *via* size exclusion chromatography (SEC) analysis in THF using polystyrene standards may be caused by the poor solubility of *trans*-rich PCOE. When cyclometalated **Ru-3a** was employed, *cis*-COE conversion reached 41%, affording PCOE with an enhanced *cis* content (42%). However, the resulting polymer was too insoluble in THF to allow for SEC analysis (Table 1, Entry 3). This result is in line with reported unsuccessful polymerizations of *cis*-COE with **Ru-3a**.^{21,22} As described in this prior study, the low strain energy of *cis*-COE is likely to blame as Grubbs and coworkers successfully polymerized *trans*-COE (with a higher ring strain energy of 16.7 kcal mol⁻¹)²⁰ with **Ru-3a** albeit with only a modest PCOE *cis* content of 70%. While previous reports have shown better *cis* contents with increasing steric bulk of the NHC ligand in cyclometalated catalysts,^{4,12} switching to bulkier **Ru-3b** bearing a 2,6-diisopropylphenyl (DIPP) ligand did not result in a higher *cis* content (Table 1, Entry 4). Moreover, only 11% conversion was achieved suggesting poorer catalyst activity, likely a result of increased steric hindrance around the Ru carbene. The somewhat surprising lack of solubility of the PCOE prepared with **Ru-3a** and **Ru-3b**—despite low monomer conversion—may suggest the formation of large polymers *via* uncontrolled ROMP. This could arise from partial catalyst initiation, leading to a small number of growing chains, and/or from the high reactivity of the 14-electron propagating carbene following the loss of the isopropoxy chelate during initiation as previously described.²¹ The persistence of the purple color characteristic of **Ru-3a** and **Ru-3b** during these polymerizations is consistent with incomplete catalyst initiation. Gratifyingly, stereoretentive dithiolate catalysts **Ru-4a** and **Ru-4b** were found to provide conversions similar to those obtained with dichloro **Ru-1** and **Ru-2**, while favoring *cis* linkages (97% and

Table 1 Catalyst screen for the ROMP of *cis*-COE



Entry	Catalyst	Time (h)	% Conv.	M_n^{theo} (kg mol ⁻¹)	M_n^{exp} (kg mol ⁻¹)	D	% <i>cis</i>
1	Ru-1	1	>99	33.1	16.2	2.36	20
2	Ru-2	1	>99	33.1	16.1	2.04	16
3	Ru-3a	24	41	13.6	— ^a	—	42
4	Ru-3b	24	11	3.7	— ^a	—	40
5	Ru-4a	1	98	32.5	107.8	1.52	97
6	Ru-4b	1	>99	33.1	66.4	1.54	72

^a The resulting polymer was too insoluble for SEC analysis in THF.



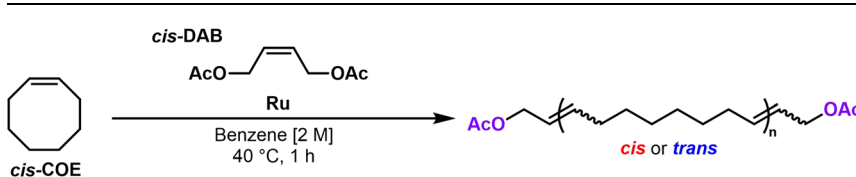
72% *cis* content, respectively; Table 1, Entries 5 and 6). Both catalysts produced polymers with significantly narrower dispersities than **Ru-1** and **Ru-2**, albeit with poor matching between predicted and experimental molar masses. Although the lower *cis*-selectivity delivered by **Ru-4b** containing a bulkier NHC remains unclear, both **Ru-4a** and **Ru-4b** were selected for the development of a catalytic stereoretentive ROMP due to their higher stereoselectivity²² and overall control compared to cyclometalated catalysts **Ru-3a** and **Ru-3b**.

Development of a catalytic stereoretentive ROMP of *cis*-COE using a functional CTA

Typical ROMP reactions require one equivalent of catalyst per polymer chain, making the process potentially costly and increasing the risk of metal contamination in the final material. Catalytic ROMP variants have been developed leveraging CTAs to shuttle Ru carbenes between growing chains. Early work by Hillmyer and Grubbs demonstrated that *cis*-DAB could be used in the ROMP of COD, enabling the efficient synthesis of telechelic polybutadiene at low catalyst loadings with high chain-end fidelity towards functionalization.^{17,23-25} Importantly, the length of the polymer in catalytic ROMP is dictated by the ratio of monomer to CTA. While other CTAs have been explored recently,²⁶⁻³⁰ we hypothesized that *cis*-DAB would be a well-suited CTA to use in combination with **Ru-4a** and **Ru-4b**, as both catalysts typically only tolerate internal alkenes and proceed through a stereoretentive mechanism, where the *cis* configuration of the olefin is retained in the product. Reaction of **Ru-4a** or **Ru-4b** with CTA *cis*-DAB would generate *in situ* an active acetoxy-functionalized initiator and cross-metathesis events following *cis*-COE polymerization would deliver all-*cis* telechelic PCOE while regenerating the Ru carbene initiator.

All initial catalytic ROMP screenings were performed under a nitrogen atmosphere at 40 °C in benzene using 150:1:0.05 monomer-to-CTA-to-catalyst

Table 2 Development of a stereoretentive catalytic ROMP of *cis*-COE



Entry	Catalyst	<i>cis</i> -COE : <i>cis</i> -DAB : Ru	% Conv.	M_n^{theo} (kg mol ⁻¹)	M_n^{exp} (kg mol ⁻¹)	D	% <i>cis</i>
1	Ru-1	150 : 1 : 0.05	>99	16.8	— ^a	—	14
2	Ru-2	150 : 1 : 0.05	>99	16.8	20.0	2.23	16
3	Ru-4a	150 : 1 : 0.05	93	15.4	18.9	1.72	97
4	Ru-4b	150 : 1 : 0.05	>99	16.8	28.7	1.62	>99
5	Ru-4b	300 : 1 : 0.05	>99	33.5	41.6	1.68	>99
6	Ru-4b	600 : 1 : 0.05	>99	66.8	85.0	1.62	>99
7	Ru-4b	1000 : 1 : 0.05	>99	111.1	127.9	1.63	>99

^a The resulting polymer was too insoluble for SEC analysis in THF.



loadings. In a typical experiment, the ruthenium catalyst was first reacted with the CTA for five minutes at 40 °C to generate the functional initiator prior to monomer addition. To minimize the formation of cyclic oligomers, all polymerizations were performed at a monomer concentration of 2 M. Since catalytic ROMP with stereoretentive catalyst has only been seldomly studied and only with norbornene derivatives that exhibit fast polymerization rates,²⁹ dichloro catalysts **Ru-1** and **Ru-2** were first used to benchmark the reaction. Catalytic ROMP using **Ru-1** resulted in a *trans*-rich polymer that was too insoluble in THF for SEC analysis (Table 2, Entry 1). **Ru-2** also led to a *trans*-rich polymer, albeit with a slightly better solubility in THF that permitted SEC analysis, which revealed a broad dispersity of 2.23 yet a good match between theoretical and experimental molar masses (Table 2, Entry 2). Switching to stereoretentive catalyst **Ru-4a** afforded a polymer with 93% conversion and 97% *cis* content with close agreement between M_n^{exp} and M_n^{theo} and a significantly narrower dispersity than **Ru-2**

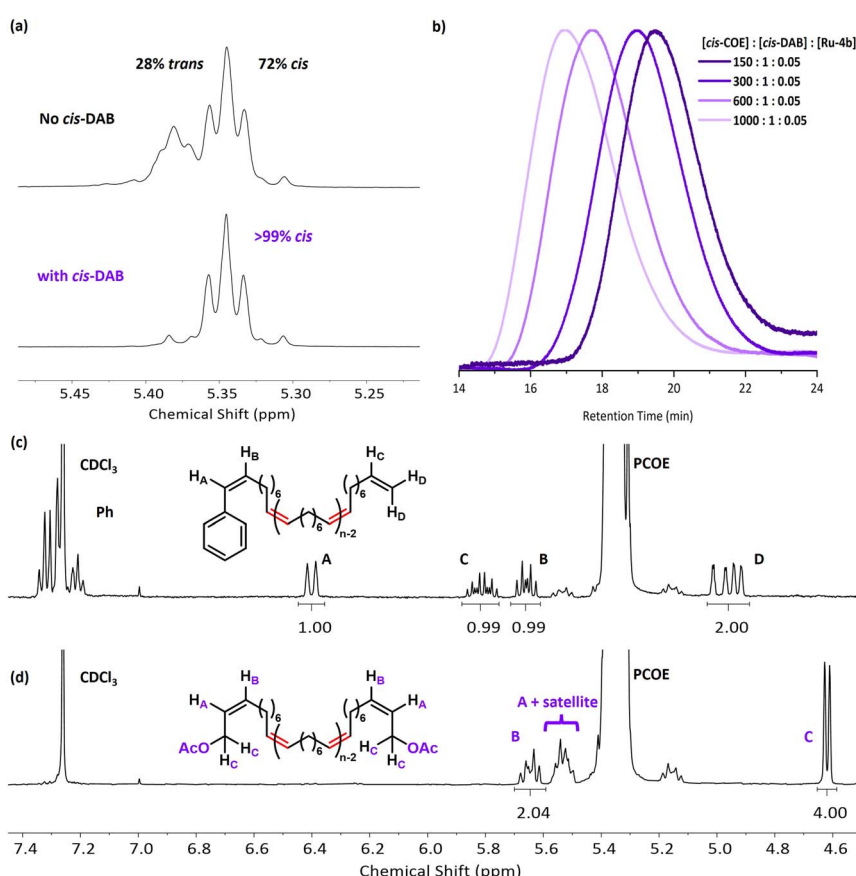


Fig. 2 (a) ^1H NMR overlay showing difference in *cis* content between conditions using 300 : 1 *cis*-COE : Ru-4b and 300 : 1 : 0.05 *cis*-COE : *cis*-DAB : Ru-4b. (b) Overlaid SEC traces for different *cis*-COE : *cis*-DAB ratios at constant Ru-4b loadings. (c) ^1H NMR analysis of chain-ends in condition using a phenyl alkylidene initiator and termination with EVE at 50 : 1 *cis*-COE : Ru-4b loading. (d) ^1H NMR analysis of functional chain-ends using 150 : 1 : 0.05 *cis*-COE : *cis*-DAB : Ru-4b.



(Table 2, Entry 3). Interestingly, **Ru-4b** led to complete *cis*-COE conversion and the resulting soluble PCOE was shown to contain only *cis* linkages (>99% *cis*) (Table 2, Entry 4), a striking difference with the 72% *cis* alkenes obtained in absence of CTA **cis**-**DAB** (Table 1, Entry 6). Although the mechanistic origin of the notable enhancement in *cis* selectivity observed with **Ru-4b** in the presence of CTA **cis**-**DAB** (Fig. 2a) remains unclear, the improved monomer conversion, higher *cis* content, and narrower dispersity prompted us to select **Ru-4b** for the remainder of the study. Predictable control over polymer molar masses was achieved with monomer-to-CTA-to-catalyst loadings up to 1000 : 1 : 0.05 (Table 2, Entries 5–7 and Fig. 2b) while maintaining >99% *cis* selectivity. The efficacy of this approach was demonstrated through the synthesis of acetoxy-functionalized, telechelic all-*cis* PCOE with an experimental M_n of 127.9 kg mol⁻¹ and complete *cis*-COE conversion after 1 hour, which was achieved using a catalyst loading 200 times lower (relative to monomer concentration) than that required by our previous *cis*-selective ADMET method that only afforded small telechelic PCOE (M_n of 3.3 kg mol⁻¹ after 48 hours).¹²

The degree of chain-end functionalization was determined through the synthesis of a smaller PCOE ($M_n^{\text{theo}} = 5.6$ kg mol⁻¹, $M_n^{\text{exp}} = 6.9$ kg mol⁻¹, $D = 2.11$, % *cis* = >99%) using a 50 : 1 monomer-to-**Ru-4b** loading and ethyl vinyl ether (EVE) as the terminating agent. Interestingly, while a shorter reaction time of only 10 minutes at this catalyst loading gave a *cis* content >99%, leaving the polymerization for 60 minutes resulted in a *cis* content of only 23%, likely suggesting isomerization due to secondary metathesis reactions in the absence of a CTA. The ¹H NMR spectrum was then compared to that of the PCOE synthesized *via* catalytic stereoretentive ROMP using a loading of 150 : 1 : 0.05 *cis*-COE : *cis*-**DAB** : **Ru-4b**. Chain-end analysis of the polymer synthesized through traditional stereoretentive ROMP with **Ru-4b** revealed chemical shifts at 5.80 and 4.95 ppm corresponding to the vinyl (=CH₂) chain-end as well as signals between 7.34–7.19, 6.40, and 5.65 ppm corresponding to the styrenyl chain-end with a 1 : 1 match of the integration values for each chain end (Fig. 2c). These assignments were also consistent with the assigned chemical shifts and integrations of a previous report using a ruthenium benzylidene initiator and ethyl vinyl ether terminating agent.³¹ Chain-end analysis of the all-*cis* PCOE synthesized *via* catalytic ROMP showed unique signals at 4.62 ppm and 5.69–5.48 ppm respectively corresponding to the acetoxy methylene and neighboring disubstituted alkenes, which is consistent with a telechelic PCOE containing identical acetoxy terminal groups (Fig. 2d). While peak overlap with the satellite peaks (¹H–¹³C coupling) of the PCOE backbone precluded accurate integration of H_a's, the integration values for H_b's and H_c's support our assignment. Careful examination of the baseline in the ¹H NMR spectrum of telechelic PCOE showed trace styrenyl and vinyl signals corresponding to a small number of chains that were either initiated by initiator **Ru-4b** rather than active functional initiator and/or terminated without the CTA (Fig. S1†). Integration analysis revealed that non-functionalized chain ends accounted for only 5% under the catalytic stereoretentive ROMP conditions, demonstrating the effectiveness of this method in producing a high proportion of telechelic polymers.



Synthesis of high molar mass all-*cis* ABA triblock copolymers

With the successful application of the catalytic stereoretentive ROPM strategy in the synthesis of high molar mass acetoxy-functionalized telechelic all-*cis* PCOE (**AcO-PCOE_{cis}-OAc**), the synthesis of all-*cis* ABA triblock copolymers through the ROP of *D,L*-lactide was targeted. To ensure good solubility of the middle block for further chain extension, **AcO-PCOE_{cis}-OAc** with an M_n^{exp} of 28.7 kg mol⁻¹ ($D = 1.62$) was selected for the subsequent hydrolysis step. Notably, the insolubility of the *trans*-rich congener after precipitation made further modification difficult, thus further underscoring the importance of enhanced processability provided by high *cis* content. Hydrolysis of **AcO-PCOE_{cis}-OAc** afforded the corresponding hydroxyl-functionalized telechelic polymer **HO-PCOE_{cis}-OH** with an expected minimal change in the molar mass distribution ($M_n^{\text{exp}} = 28.8$ kg mol⁻¹, $D = 1.52$) according to SEC analysis (Fig. 3a). Complete hydrolysis of **AcO-PCOE_{cis}-OAc** was confirmed through ¹H NMR analysis (see ESI Fig. S2†). Inspired by the work of Hedrick and Waymouth,^{32–35} triazabicyclodecene (TBD) and diazabicycloundecene (DBU) were tested for the ROP of *D,L*-lactide from macroinitiator **HO-PCOE_{cis}-OH** using a ratio of *D,L*-lactide to **HO-PCOE_{cis}-OH** of 1000 : 1. **HO-PCOE_{cis}-OH** ($M_n^{\text{exp}} = 28.8$ kg

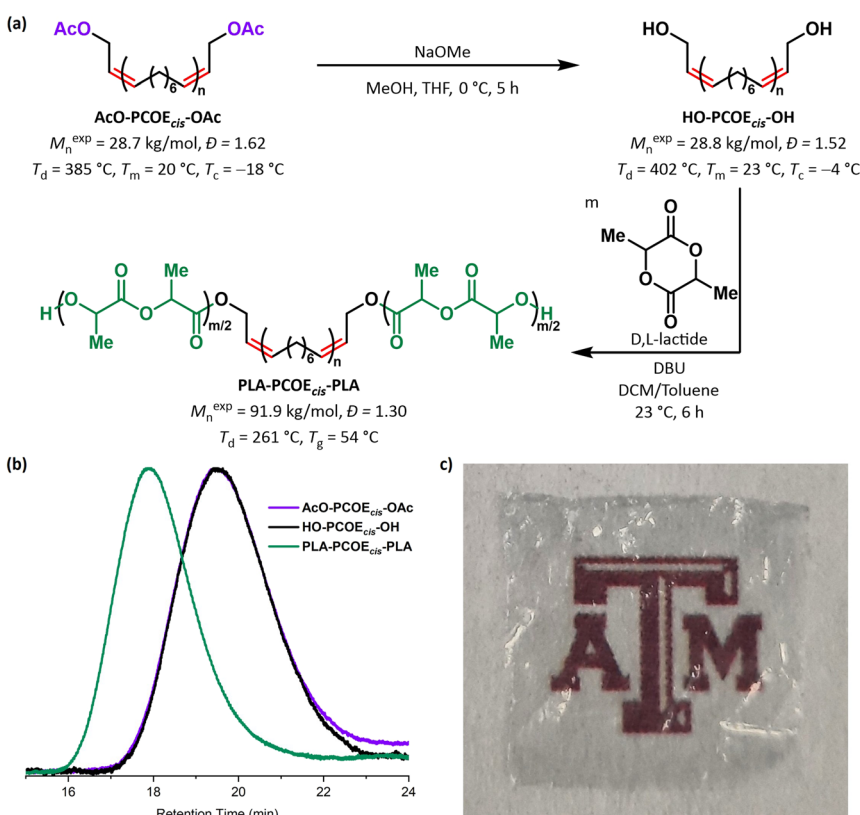


Fig. 3 (a) Synthesis of **PLA-PCOE_{cis}-PLA** and corresponding thermal data. (b) SEC traces showing successful chain extension after ROP of *D,L*-lactide. (c) A plastic thin film of **PLA-PCOE_{cis}-PLA** ($M_n^{\text{exp}} = 105.0$ kg mol⁻¹, $D = 1.28$) prepared through solvent casting.



mol^{-1}) was observed to have better solubility in toluene, while D,L-lactide was significantly more soluble in DCM, so a 1 : 1 mixture of the two solvents was used in the optimized reaction conditions. While both organocatalysts afforded high monomer conversion (98%), DBU delivered PLA end blocks ($M_n^{\text{exp}} = 91.9 \text{ kg mol}^{-1}$, $D = 1.30$ vs. $M_n^{\text{exp}} = 65.7 \text{ kg mol}^{-1}$, $D = 1.27$ for TBD) closer to the expected value ($M_n^{\text{exp}} = 172.9 \text{ kg mol}^{-1}$) (Fig. 3b). PLA homopolymerization initiation and/or premature termination by adventitious water trace likely explained the lower obtained molar masses.^{36,37}

The thermal properties of the synthesized **PLA-PCOE_{cis}-PLA** triblock copolymer, along with those of the precursor homopolymers, were characterized using thermal gravimetric analysis (TGA) and differential scanning calorimetry (DSC). These properties were then compared to analogous polymers with smaller molar masses obtained previously with our *cis*-selective ADMET strategy.¹² In addition to higher thermal decomposition temperatures (T_d measured at 5% mass loss) for the larger molar mass **AcO-PCOE_{cis}-OAc** and **HO-PCOE_{cis}-OH**, the melting temperature (T_m) for **AcO-PCOE_{cis}-OAc** increased by 31 °C ($T_m = -9 \text{ }^{\circ}\text{C}$ for 3.3 kg mol $^{-1}$ vs. $T_m = 20 \text{ }^{\circ}\text{C}$ for 28.7 kg mol $^{-1}$) while the crystallization transition temperature (T_c) of **HO-PCOE_{cis}-OH** increased by 35 °C ($T_c = -39 \text{ }^{\circ}\text{C}$ for 3.3 kg mol $^{-1}$ vs. $T_c = -4 \text{ }^{\circ}\text{C}$ for 28.8 kg mol $^{-1}$). The larger polymers exhibited T_m 's near room temperature, consistent with their physical appearance reversibly transitioning from a solid to a highly viscous melt under ambient conditions. Finally, the glass transition temperature (T_g) of **PLA-PCOE_{cis}-PLA** increased by 22 °C with larger molar mass ($T_g = 32 \text{ }^{\circ}\text{C}$ for 17.3 kg mol $^{-1}$ vs. $T_g = 54 \text{ }^{\circ}\text{C}$ for 91.9 kg mol $^{-1}$), a promising feature in packaging and fibers where a more rigid material is required over a broader temperature range. In addition to investigating thermal properties, nanoindentation was used to determine the E_r and hardness (H) of the material using the standard Oliver and Pharr analysis from the unloading segments of the load–displacement curves.³⁸ Scaling up the triblock copolymer synthesis provided **PLA-PCOE_{cis}-PLA** with an $M_n^{\text{exp}} = 105.0 \text{ kg mol}^{-1}$ and $D = 1.28$ which had an H of 0.137 GPa and E_r of 3.55 GPa. While the E_r was slightly higher than the smaller analogous triblock ($M_n^{\text{exp}} = 17.3 \text{ kg mol}^{-1}$, $D = 1.32$, $H = 0.138 \text{ GPa}$, $E_r = 3.0 \text{ GPa}$), both the H and E_r were still significantly lower than PLA ($M_n^{\text{exp}} = 19.9 \text{ kg mol}^{-1}$, $D = 1.72$, $H = 0.19 \text{ GPa}$, $E_r = 4.7 \text{ GPa}$), indicating a lower stiffness of the material.¹² Solvent casting of **PLA-PCOE_{cis}-PLA** afforded a transparent plastic thin film, further demonstrating the potential of the material for packaging applications (Fig. 3c). Importantly, the hydrolytic lability of PLA enabled the recovery of the middle all-*cis* PCOE block, which suggests that this ABA triblock strategy would maintain the chemical recyclability of PLA.^{39,40}

Conclusions

In summary, a catalytic stereoretentive ROMP strategy has been developed for synthesizing high molar mass all-*cis* PCOE and PLA-terminated ABA triblock copolymers. Screening of various types of Ru-carbenes revealed that stereoretentive dithiolate ruthenium **Ru-4a** and **Ru-4b** outperformed *cis*-selective cyclometalated catalysts **Ru-3a** and **Ru-3b** in the ROMP of *cis*-COE, affording higher monomer conversion, enhanced control over propagation, and superior *cis*-stereoselectivity. Interestingly, a more controlled ROMP was achieved in the presence of CTA **cis**-DAB enabling the preparation of *cis*-PCOE with tunable molar



masses as a function of monomer-to-CTA ratio. The use of CTA *cis*-DAB enabled high-fidelity functionalization at both chain ends and the isolation of acetoxy-terminated telechelic PCOE featuring >99% *cis* alkenes and unprecedented molar masses up to 127.9 kg mol⁻¹—achieved at catalyst loadings 200 fold lower than those required in our previously reported *cis*-selective ADMET strategy. Subsequent hydrolysis followed by chain extension through the ROP of D,L-lactide with DBU as an organocatalyst allowed the synthesis of high molar mass all-*cis* ABA triblock copolymers with an M_n^{exp} up to 105.0 kg mol⁻¹. Notably, a 22 °C increase in T_g was observed in the larger triblock copolymer, in addition to a lower stiffness compared to PLA as measured through nanoindentation.

Data availability

The data supporting this article have been included as part of the ESI.†

Author contributions

J. L. N. and Q. M. conceived the work. J. L. N. and A. C. G. conducted experimental work and all authors analyzed the data. Q. M. supervised the work. J. L. N. wrote the initial draft of the work which was edited through contributions of all authors. All authors have given approval to the final version of the manuscript.

Conflicts of interest

There are no conflicts to declare.

Acknowledgements

This work was performed at Texas A&M University with support from the National Science Foundation (CHE-2238888) and the Welch Foundation (A-2204-20240404). Use of the NMR facility in the Department of Chemistry, Materials Characterization Core Facility (RRID:SCR_022202), and Soft Matter Facility (RRID:SCR_022482) are acknowledged. The authors would like to thank Umicore for the generous donation of metathesis catalysts, Srutashini Das (TAMU) for technical help with nanoindentation film preparation, and Dr Wilson Serem (TAMU) for his technical expertise in nanoindentation. J. L. N. acknowledges the support from the Hagler Institute for Advanced Study through a HEEP graduate fellowship and Q. M. thanks the Camille and Henry Dreyfus Foundation for support *via* the Camille Dreyfus Teacher-Scholar Award (TC-24-059).

Notes and references

- 1 K. Endo and R. H. Grubbs, *J. Am. Chem. Soc.*, 2011, **133**, 8525–8527.
- 2 B. K. Keitz, K. Endo, M. B. Herbert and R. H. Grubbs, *J. Am. Chem. Soc.*, 2011, **133**, 9686–9688.
- 3 B. K. Keitz, K. Endo, P. R. Patel, M. B. Herbert and R. H. Grubbs, *J. Am. Chem. Soc.*, 2012, **134**, 693–699.
- 4 M. S. Mikus, S. Torker and A. H. Hoveyda, *Angew. Chem., Int. Ed.*, 2016, **55**, 4997–5002.



5 R. K. M. Khan, S. Torker and A. H. Hoveyda, *J. Am. Chem. Soc.*, 2013, **135**, 10258–10261.

6 T.-W. Hsu, C. Kim and Q. Michaudel, *J. Am. Chem. Soc.*, 2020, **142**, 11983–11987.

7 S. J. Kempel, T.-W. Hsu and Q. Michaudel, *Synlett*, 2021, **32**, 851–857.

8 T.-W. Hsu, S. J. Kempel and Q. Michaudel, *J. Polym. Sci.*, 2022, **60**, 569–578.

9 H. Mandal, O. J. Ogunyemi, J. L. Nicholson, M. E. Orr, R. F. Lalisse, Á. Rentería-Gómez, A. R. Gogoi, O. Gutierrez, Q. Michaudel and T. Goodson III, *J. Phys. Chem. C*, 2024, **128**, 2518–2528.

10 Q. Michaudel, S. J. Kempel, T.-W. Hsu and J. N. deGruyter, in *Comprehensive Organometallic Chemistry IV*, ed. G. Parkin, K. Meyer and D. O'Hare, Elsevier, Oxford, 2022, pp. 265–338.

11 T.-W. Hsu, S. J. Kempel, A. P. Felix Thayne and Q. Michaudel, *Nat. Chem.*, 2023, **15**, 14–20.

12 S. J. Kempel, T.-W. Hsu, J. L. Nicholson and Q. Michaudel, *J. Am. Chem. Soc.*, 2023, **145**, 12459–12464.

13 E. T. H. Vink, K. R. Rábago, D. A. Glassner, B. Springs, R. P. O'Connor, J. Kolstad and P. R. Gruber, *Macromol. Chem. Phys.*, 2004, **4**, 551–564.

14 K. S. Anderson, K. M. Schreck and M. A. Hillmyer, *Polym. Rev.*, 2008, **48**, 85–108.

15 S. Jacobsen and H. G. Fritz, *Polym. Eng. Sci.*, 1999, **39**, 1303–1310.

16 M. Hiljanen-Vainio, P. Varpomaa, J. Seppälä and P. Törmälä, *Macromol. Chem. Phys.*, 1996, **197**, 1503–1523.

17 L. M. Pitet and M. A. Hillmyer, *Macromolecules*, 2009, **42**, 3674–3680.

18 Sigma-Aldrich, Hoveyda-Grubbs Catalyst® M2001, 2 g = \$1,880.00, https://www.sigmaaldrich.com/US/en/product/aldrich/771082?srsltid=AfmBOorY9KB5QqlLiicLx27bx7KBxpP_tx9EsZ9V47KYCcj9RCJWlfeu, last accessed May 2nd, 2025.

19 Sigma-Aldrich, Grubbs Catalyst® M204, 2 g = \$267.00, <https://www.sigmaaldrich.com/US/en/product/aldrich/569747?srsltid=AfmBOorDSBHBmv7qCxDlVkwL34755XW1VD36EuGdp0AUuS1dD0BCpoJ>, last accessed May 2nd, 2025.

20 H. Martinez, N. Ren, M. E. Matta and M. A. Hillmyer, *Polym. Chem.*, 2014, **5**, 3507–3532.

21 B. K. Keitz, A. Fedorov and R. H. Grubbs, *J. Am. Chem. Soc.*, 2012, **134**, 2040–2043.

22 A. K. Rylski, H. L. Cater, K. S. Mason, M. J. Allen, A. J. Arrowood, B. D. Freeman, G. E. Sanoja and Z. A. Page, *Science*, 2022, **378**, 211–215.

23 M. A. Hillmyer and R. H. Grubbs, *Macromolecules*, 1993, **26**, 872–874.

24 M. A. Hillmyer, S. T. Nguyen and R. H. Grubbs, *Macromolecules*, 1997, **30**, 718–721.

25 C. W. Bielawski, D. Benitez, T. Morita and R. H. Grubbs, *Macromolecules*, 2001, **34**, 8610–8618.

26 P. Liu, M. Yasir, A. Ruggi and A. F. M. Kilbinger, *Angew. Chem., Int. Ed.*, 2018, **57**, 914–917.

27 M. Yasir, P. Liu, I. K. Tennie and A. F. M. Kilbinger, *Nat. Chem.*, 2019, **11**, 488–494.

28 I. Mandal, A. Mandal, M. A. Rahman and A. F. M. Kilbinger, *Chem. Sci.*, 2022, **13**, 12469–12478.



29 I. Mandal and A. F. M. Kilbinger, *J. Am. Chem. Soc.*, 2024, **146**, 32072–32079.

30 I. Mandal and A. F. M. Kilbinger, *Angew. Chem., Int. Ed.*, 2024, **63**, e202409781.

31 X. Wang, Y. Xu and J. Wang, *Angew. Chem., Int. Ed.*, 2024, **63**, e202409534.

32 N. E. Kamber, W. Jeong, R. M. Waymouth, R. C. Pratt, B. G. G. Lohmeijer and J. L. Hedrick, *Chem. Rev.*, 2007, **107**, 5813–5840.

33 M. K. Kiesewetter, E. J. Shin, J. L. Hedrick and R. M. Waymouth, *Macromolecules*, 2010, **43**, 2093–2107.

34 R. C. Pratt, B. G. G. Lohmeijer, D. A. Long, R. M. Waymouth and J. L. Hedrick, *J. Am. Chem. Soc.*, 2006, **128**, 4556–4557.

35 B. G. G. Lohmeijer, R. C. Pratt, F. Leibfarth, J. W. Logan, D. A. Long, A. P. Dove, F. Nederberg, J. Choi, C. Wade, R. M. Waymouth and J. L. Hedrick, *Macromolecules*, 2006, **39**, 8574–8583.

36 F. E. Kohn, J. W. A. Van Den Berg, G. Van De Ridder and J. Feijen, *J. Appl. Polym. Sci.*, 1984, **29**, 4265–4277.

37 R. D. Lundberg, J. V. Koleske and K. B. Wischmann, *J. Polym. Sci., Part A: Polym. Chem.*, 1969, **7**, 2915–2930.

38 W. C. Oliver and G. M. Pharr, *J. Mater. Res.*, 1992, **7**, 1564–1583.

39 V. Piemonte, S. Sabatini and F. Gironi, *J. Polym. Environ.*, 2013, **21**, 640–647.

40 T. M. McGuire, A. Buchard and C. Williams, *J. Am. Chem. Soc.*, 2023, **145**, 19840–19848.

